Rare Met. (2021) 40(9):2354–2368
https://doi.org/10.1007/s12598-021-01727-y

RARE METALS

REVIEW

Noble metal-based high-entropy alloys as advanced electrocatalysts for energy conversion

Yu-Chen Qin*, Feng-Qi Wang, Xin-Ming Wang, Ming-Wei Wang*, Wen-Long Zhang, Wan-Kai An, Xiao-Peng Wang*, Yun-Lai Ren, Xin Zheng, Dong-Can Lv, Ayyaz Ahmad

Received: 23 November 2020 / Revised: 14 December 2020 / Accepted: 17 December 2020 / Published online: 28 April 2021

Abstract Noble metal-based high-entropy alloy nanoparticles (NM-HEA NPs) have exhibited brilliant catalytic performance toward electrocatalytic energy conversion and attracted increasing attention. The near-equimolar mixed elements of NM-HEA NPs may result in the unique properties including cocktail effect, high entropy effect and lattice distortion effect, which are beneficial for improving the catalytic performance and reducing the amount of noble metal. Herein, several advanced NM-HEA NPs as electrocatalysts for energy conversion are systematically summarized. The preparation methods of NM-HEA NPs are evaluated as well as the catalytic properties and mechanism are discussed classified by electrocatalytic reactions. Finally, the challenges and prospects in this field are carefully discussed. This review provides an overview on recent advances of NM-HEA electrocatalysts for energy conversion and draws more attention in this infant research field.

Keywords Noble metal-based high-entropy alloys; Electrocatalysis; Energy conversion; Synthesis; Catalytic performance

1 Introduction

The development of green energy conversion technologies has been strongly desired as the ever-increasing energy crisis and environmental pollution caused by the excessive consumption of traditional fossil fuels [1]. Electrocatalytic energy conversion technology (EECT), such as water electrolysis, fuel cells, electrochemical nitrogen fixation and electrochemical reduction of CO_2, has attracted extensive attention and exhibited great application potential due to the higher conversion efficiency and less carbon emissions [2–7]. However, most of the efficient electrocatalysts for EECT are noble metal-based nanoparticles (NPs). The high cost, low reserves and unsatisfactory performance of these noble metal-based electrocatalysts have been the main bottlenecks that limit the large-scale practical applications [8–12]. Therefore, over the past decades, numerous efforts focused on boosting the catalytic property and reducing the cost of electrocatalysts toward EECT. Among them, alloying noble metals with transition metals is a promising technology. A lot of binary and ternary alloyed noble metal-based electrocatalysts with lower noble metals contents have exhibited outstanding catalytic performance [13–22].

High-entropy alloys (HEAs) were first reported in 2004, which are defined based on the component as

Y.-C. Qin*, F.-Q. Wang, W.-L. Zhang, W.-K. An, X.-P. Wang*, Y.-L. Ren, X. Zheng, D.-C. Lv
College of Sciences, Henan Agricultural University, Zhengzhou 450000, China
e-mail: qinyuchen@henau.edu.cn

X.-P. Wang
e-mail: xpwang@henau.edu.cn

X.-M. Wang, M.-W. Wang*
State-Key Laboratory of Chemical Engineering, and Shanghai Key Laboratory of Multiphase Materials Chemical Engineering, East China University of Science and Technology, Shanghai 200237, China
e-mail: mingweiwang@ecust.edu.cn

A. Ahmad
Department of chemical Engineering MNS University of Engineering and Technology, Multan 60000, Pakistan

alloys with five or more principal elemental components in equimolar ratios (another definition is an atomic concentration between 5% and 35%). The definition of HEAs is still controversial, and some argue that there is no need to limit the concentration of elements [23, 24]. Besides, HEAs were also defined by mixed configuration entropy (S), and S can be calculated by the following formulas:

$$S = -R\sum x_i \cdot \ln x_i \quad (1)$$

$$S = R\ln n \quad (2)$$

where R stands for the molar gas constant, x_i is the mole fraction of the elemental component and n represents the amount of composition in the alloy. And when $S \geq 1.36\ R$, the HEA is turned out be a quaternary alloy; when $S \geq 1.5\ R$, the HEA is composed of more than five elements [25]. After more than a decade of research, HEAs have shown many fascinating properties and attracted numerous attentions. However, most of the researches have paid close attention to the mechanical property including elasticity modulus, shearing modulus, hardness and strength of extension [26–30]. The chemical property of HEAs has been studied rarely. Recently, HEAs as a novel electrocatalyst for EECT have begun to draw attention. The influence of HEAs properties and characteristics on catalytic performance has been investigated from experimental and theoretical calculations [31, 32].

Compared to binary and ternary alloys, HEAs generally have more advantages in catalytic field, such as cocktail effect, high entropy effect, lattice distortion effect, phase structure and sluggish diffusion effect [24, 33]. Cocktail effect means synergistic response among the alloys with various elemental components, which could be tuned by changing the component elements of HEAs. This cocktail effect could effectively modify the electronic structure such as d-band center, which directly manages the adsorption and activation of reactants and intermediates, determining the catalytic performance of HEAs. Surface environment of HEAs such as surface charge distribution could also be governed by modulating the cocktail effect, which affects the adsorption of reactants and thereby improves the catalytic performance [34]. Moreover, HEAs have a higher degree of mixed configuration relative to that of binary and ternary alloys, which named high entropy effect. Benefiting from the high entropy effect, HEAs usually have a stronger corrosion and oxidation resistance and lower atomic diffusion rate, resulting in a more stable structure and catalytic stability of HEAs [35, 36]. Lattice distortion existing widely in HEAs due to the various atomic sizes of each elemental component, usually the surface strain effect. Fine-tuning the surface strain of electrocatalysts could effectively regulate their d-band center according to the previous reports [37–39]. In general, the downshift of d-band center will reduce the adsorption capacity of reactants and intermediates, while the upshift of d-band center will result in a strong interaction [40–42]. Therefore, taking advantages of lattice mismatch in HEAs may become a powerful strategy to boost the electrocatalytic performance. Phase structure also plays a significant important role in determining the property of HEAs. The simple phases such as face-centered cubic (fcc), body-centered cubic (bcc) and hexagonal close packed (hcp) are highly associated with their catalytic performance [43–47]. Therefore, controlling the phase structure of HEAs can bring unexpected effect to improve the catalytic performance. Especially in recent studies, fabricating HEAs with desirable mixed-phase could dramatically enhance the catalytic property. Although noble metals have excellent catalytic properties in electrocatalytic reactions, they are not stable enough usually. After forming HEAs, the stability will be greatly enhanced. Owing to the large difference in the atomic size of HEAs, the lattice distortion effect will increase the energy barrier of atom diffusion and hinder the atomic diffusion, which will lead to the sluggish diffusion effect of HEAs. The sluggish diffusion effect and high entropy effect are the main reasons for the HEAs to remain stable in acidic or alkaline environments.

In this review, we focus on the recent research on noble metal-based HEAs (NM-HEAs) electrocatalysts for EECT. The synthetic methods of NM-HEAs are systematically summarized firstly. Then we discuss the catalytic performance and mechanism of NM-HEAs in detail according to the various electrocatalytic reactions through experimental and theoretical calculations. Finally, the challenges, opportunities and development tendency in this field are proposed to the authors' knowledge.

2 Fabrication and detection of NM-HEA NPs

At the early stage, most studies on HEA have focused on macroscopic HEA materials or bulk solids, which could be obtained by mechanical alloying [48, 49], vacuum smelting [50], powder metallurgic [51] or electrochemical deposition method [52]. However, these methods have difficulty in constructing nano-sized NM-HEA materials [53]. The key problem is the tradition method tends to form nanocrystals with separated phases rather than alloys. Especially once the elements exceed three, the rates of nucleation and growth decrease due to the reduced substitutional diffusion and interaction among the inter-diffusing species during partitioning [54]. Therefore, developing rational method to construct a stable single-

phase solid solution structure consisting of more than five elements is highly desirable.

2.1 Top-to-down methods

2.1.1 Mechanical alloying at low temperatures

NM-HEA bulk solids are prepared firstly and milled at 123 K via the single ball cryomilling (Fig. 1a) after several hours to obtain NPs, such as CuAuAgPtPd. Kumar et al. [55] used this method to synthesize $Cu_{0.2}Ag_{0.2}Au_{0.2}Pt_{0.2}Pd_{0.2}$, which has higher product quality and finer powder than other methods. The cryomilling not only has the advantages of high yield and purity, fine powder, keeping the atomic composition of NM-HEAs and reducing air pollution, but also has the great superiority of large-scale preparation of high-entropy alloy NPs, which has attracted wide attention.

2.1.2 Spark discharge

NM-HEA bulk solids prepared were used as the electrode in spark discharge system (Fig. 1b). Wu et al. [56] synthesized CoCrFeNiPt and $CoFeNiCr_{0.5}Pd_{0.8}$ with uniform elemental distribution by the spark discharge way. Under direct current (DC) pulse power of 500 W and pulse width of 50 μs with a duty ratio of 0.5, atoms of different elements on the HEA electrodes are evaporated, and then recondensed into NPs after encountering the cold water to form HEA NPs.

2.2 Down-to-top methods

2.2.1 Electrodeposition based on nanodroplet-mediation

Glasscott et al. [57] synthesized CoFeLaNiPt high-entropy metallic glasses (HEMGs) by electrodeposition of metal

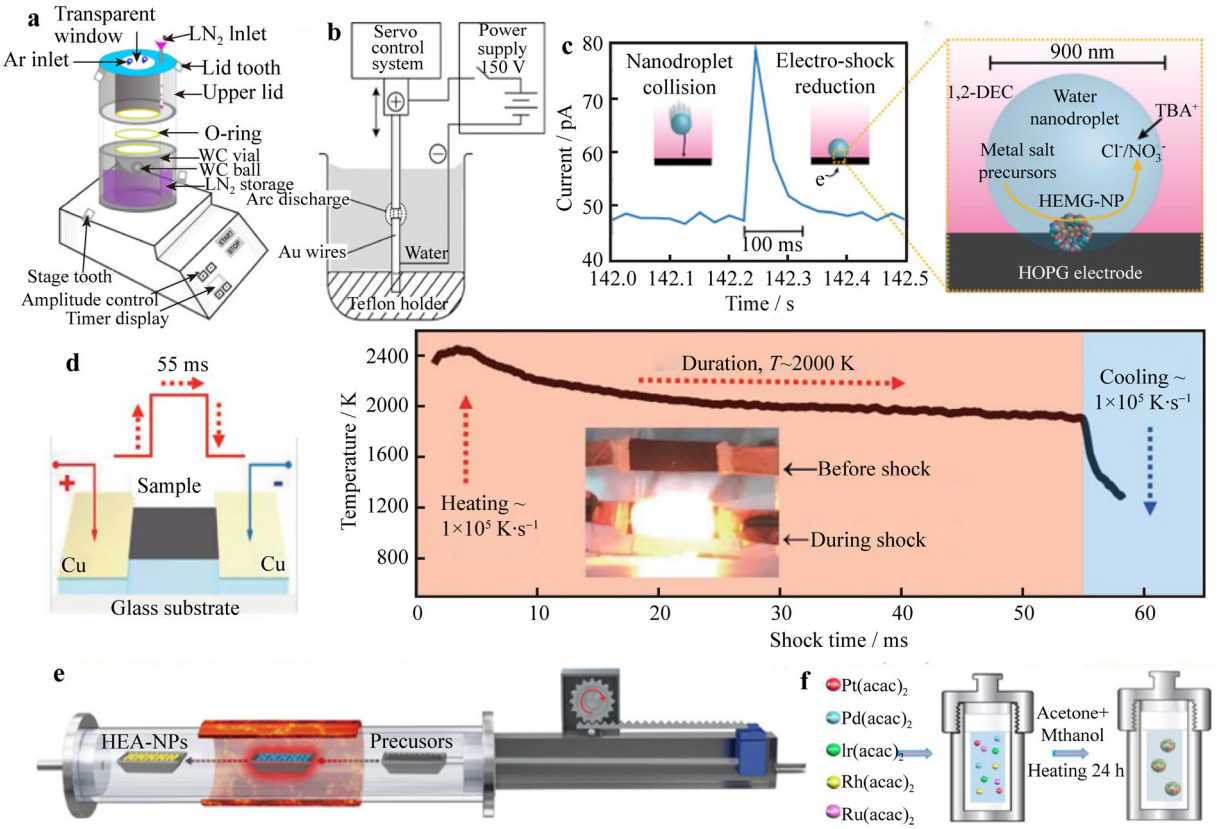

Fig. 1 **a** Customized single ball cryomill (WC-tungsten carbide) diagram. Reproduced with permission from Ref. [55]. Copyright 2018, Springer. **b** General DC arc discharge system composes of above parts. Reproduced with permission from Ref. [56]. Copyright 2018, Springer. **c** Diagram on left showing relationship between transient current and time generated by collision of a single nanodroplet on carbon fiber, and diagram on right showing a detailed description of collision process of nanodroplet. Reproduced with permission from Ref. [57]. Copyright 2019, Nature Publishing Group. **d** Schematic diagram of sample preparation and temperature versus time during 55-ms thermal shock. Reproduced with permission from Ref. [53]. Copyright 2018, American Association for the Advancement of Science. **e** Experimental diagram for synthesis of HEA NPs by fast-moving bed pyrolysis (FMBP). Reproduced with permission from Ref. [60]. Copyright 2020, Nature Publishing Group. **f** Process diagram of HEAs synthesis by solvent-thermal method. Reproduced with permission from Ref. [25]. Copyright 2020, American Chemical Society

salt precursors onto a conductive surface. Metal salt precursors firstly are dissolved water, and then suspended in dichloroethane to form nanodroplet with assisting of tetrabutylammonium perchlorate and ultrasonic. Delivery of the precursor atoms to the substrate results from the collision of nanodroplets with a biased electrode represents an electro-shock event on the order of 100 ms, rapidly reducing up to eight confined metal salt precursors into HEA NPs with precisely tunable stoichiometric ratios (Fig. 1c). Nanodroplet-mediated electrodeposition is an ideal method used to form HEMG-NPs at room temperature, which can maintain precise control over elemental stoichiometry.

2.2.2 Carbothermal shock (CTS)

Yao et al. [53] utilized CTS method to synthesize PtPdCoNiFeCuAuSn in 2018. In CTS, different metal salt mixtures (Pt, Pd, Ni, Fe, Co, Au, Cu, Sn, etc.) are first loaded onto the carbon support, such as carbon fiber. Then, flash heating is employed to trigger the rapid thermal decomposition of the metal salt at high temperature (about 2000 K, with impact duration of 55 ms and rate about 105 $K{\cdot}S^{-1}$) (Fig. 1d), forming small droplets of multimetallic solution. Following, these droplets are rapidly cooled to form a uniform and homogeneous HEA NP without aggregation or phase separation. Through controlling the CTS parameters (substrate, temperature, impact duration and heating/cooling rate), new types of NPs with different structures and different practical values could be prepared. The maximum temperature of the carbothermal method is high enough to promote uniform mixing of almost any metal combination.

2.2.3 Ultrasonication-assisted wet chemistry

Liu et al. [58] reported an ultrasonication-assisted wet chemistry method for preparing noble AuRuRhPdPt HEA NPs, utilizing the acoustic cavitation phenomenon in ultrasonication process in which extremely high temperatures in localized microscopic regions at momentary timespans were derived (up to $\sim$5000 °C of temperature and $\sim 2.03 \times 10^8$ Pa of pressure were generated in localized microscopic regions at a time scale of less than 1×10^{-9} s). The metal salt could be co-reduced by reducing agents and transform to alloy structures under operation. Compared with other wet chemistry methods, this technology uses ultrasonic technology to produce multimetallic alloy NPs with smaller particle sizes.

2.2.4 Fast cooling and dealloying

Qiu et al. [59] reported the construction of nanoporous AlNiFeCoCuMoPdPtAu HEA NPs by precursor fast cooling and dealloying. The bulk HEA solid is first prepared by melting pure melts using an induction-melting furnace under Ar protection, followed by spinning to prepare the alloy ribbons. Later, the ribbons are immersed in 0.5 $mol{\cdot}L^{-1}$ NaOH solution for chemical dealloying to prepare the nanoporous high-entropy alloys (np-HEAs). Compared with other high-entropy alloys, np-NM-HEAs not only reduce the content of noble metals, but also greatly improve their electrochemical activity and stability, making them more widely used in sensing and energy storage.

2.2.5 Fast-moving bed pyrolysis method

Recently, a strategy that through pyrolysis of metal salt precursor loaded on carbon supports in fast-moving bed to form ultrasmall and highly dispersed MnCoNiCuRhPdSnIrPtAu HEA NPs, was investigated by Gao et al. [60]. Fast pyrolysis of precursors at high temperatures results in the formation of HEA NPs due to the low free energy of the formation of nuclei (Fig. 1e). Moreover, after formation, the HEA NPs are directly dispersedly immobilized on granular supports for industrial applications.

2.2.6 Solvothermal synthesis

Solvothermal method is one of the most commonly used methods to prepare noble metal-based NPs. In previous reports, this method has also been employed to fabricate NM-HEAs. Bondesgaard et al. [61] reported a low-temperature solvothermal autoclave synthesis method at 200 °C with a reaction duration of 4–24 h in Teflon-lined steel autoclave. Metal salt precursor solutions are first dissolved in a mixture of acetone-ethanol (50:50 vol%), and then the solution is transferred to Teflon-lined steel autoclave which allows the chemical reaction taking place in a nonaqueous solvent at temperature above the boiling point and pressures above 1×10^5 Pa, to form RuRhPdIrPt HEA NPs (Fig. 1f). Wu et al. [62] successfully prepared NM-HEAs with all six Pt group elements through co-reduction process. The mixture of six metal precursors was dissolved in water, then added dropwise to the preheated TEG/PVP solution with 230 °C at a speed of 2 $ml{\cdot}min^{-1}$. After the solution was cooled to room temperature, NM-HEAs with the size of 3 nm were obtained.

2.3 Main characteristic methods of detecting element composition

HEAs are composed of many kinds of elements, the kinds, distribution and content of elements should be confirmed when testing its properties. There are many detection methods to determine the element compositions, such as X-ray diffraction (XRD), X-ray fluorescence (XRF), X-ray photoelectron spectroscopy (XPS). XRD can determine whether the sample is amorphous or crystal according to the measured diffraction information. By comparing with the standard pattern, we can also know what composition the sample contains. XRF is an analytical method that measures elements from Na to U in the periodic table. The analytical method can be used for qualitative and quantitative analysis without destroying the sample, but it is easy to be affected by mutual element interference and superposition peak. XPS can be used not only for qualitative analysis of elements, but also for quantitative analysis of elements. In qualitative analysis, almost all elements except H and He can be identified according to the position of the characteristic spectral line in the energy spectrum. Inductively coupled plasma optical emission spectrometer (ICP-OES), also known as inductively coupled plasma atomic emission spectrometer (ICP-AES) and inductively coupled plasma mass spectrometry (ICP-MS) can detect most elements in the periodic table, but the detection ability of the latter is higher than that of the former.

3 NM-HEAs for electrocatalysis

In recent years, several efforts have focused on application of NM-HEAs for advanced electrocatalysts toward various energy conversion reactions including liquid fuel oxidation reaction (FOR), oxygen reduction reaction (ORR), hydrogen evolution reaction (HER), oxygen evolution reaction (OER) and CO_2 reduction reaction (CO_2RR). Based on experimental results and theoretical calculations, NM-HEAs electrocatalysts have exhibited great promising on the enhancement of catalytic activity and stability.

3.1 Electrocatalytic FOR

Proton exchange membrane fuel cells (PEMFCs) have attracted numerous attentions for several decades due to the high energy conversion efficiency, pollution-free process and portability [63–65]. Besides hydrogen energy, some organic small molecules such as methanol, ethanol and formic acid could also be regarded as ideal liquid fuel used in the anode of fuel cells for oxidation reaction. Pt-based nanostructured catalysts are the most efficient electrocatalysts for liquid FOR [66–70]. However, the high cost, low tolerance of CO and unsatisfactory structural stability hinder its broad applications [71]. In recent studies, Pt-based HEAs exhibit great potential to improve the catalytic performance and structured stability. Wu et al. [62] fabricated the platinum-group metals HEAs (PEG-HEA) with six elements through a facile wet chemical method. These PEG-HEA NPs with the average size of 3.1 nm are uniformly dispersed. The energy-dispersive X-ray spectroscopy (EDX) elemental mapping images reveal the homogeneous distribution of Ru, Rh, Pd, Os, Ir and Pt in the PEG-HEA NPs (Fig. 2a). The composition of PEG-HEA NPs was detected by XRF and XPS. Both results reveal that each element has a ratio of 1%–20% (Fig. 2b), indicating the successful synthesis of HEAs. These PEG-HEA NPs were evaluated as anodic electrocatalysts for ethanol oxidation reaction (EOR) and showed the superior specific and mass activity, indicating the complex 12-electron transfer processes (Fig. 2c–f). This excellent performance of EOR could be attributed to the ideal adsorption/desorption sites provided by the multielement surface of PEG-HEA NPs. Besides EOR, NM-HEAs also have been investigated as electrocatalysts for methanol oxidation reaction (MOR). Li and co-workers synthesized PdNiCoCuFe high-entropy alloyed nanotube arrays (NTAs) through template-assisted electrodeposition method (Fig. 2g) [72]. The content of each element in PdNiCoCuFe NTAs is between 9 at% and 33 at%, which is corresponding to the definition of HEAs. Owing to the high entropy effect and unique structure, PdNiCoCuFe NTAs show higher catalytic activity than commercial Pd/C catalyst with lower Pd content, as well as the excellent tolerance of CO (Fig. 2h, i). Moreover, Zhang and co-workers prepared PtRuCuOsIr catalyst with abundant nanoporous by a mild chemical dealloying method [73]. Compared to commercial Pt/C, PtRuCuOsIr catalyst exhibited enhanced catalytic activity and stability for MOR. These studies indicate that preparing NM-HEAs catalysts is an effective strategy to reduce the content of noble metal and improve the catalytic performance toward liquid FOR.

3.2 Electrocatalytic ORR

The sluggish kinetics and complex multielectron process of ORR have become a key constraint on improving the efficiency of fuel cell. Therefore, designing and fabricating outstanding electrocatalysts toward ORR has been strongly desired and attracted numerous attentions in recent decades. Until now, a lot of state-of-art catalysts especially noble metal-based catalysts have been obtained [8, 12, 22, 74–79]. But the problems of high noble metal usage and unsatisfactory catalytic activity and stability remained. Recently, based on theoretical calculations and experiments, NM-HEAs catalysts have shown a great

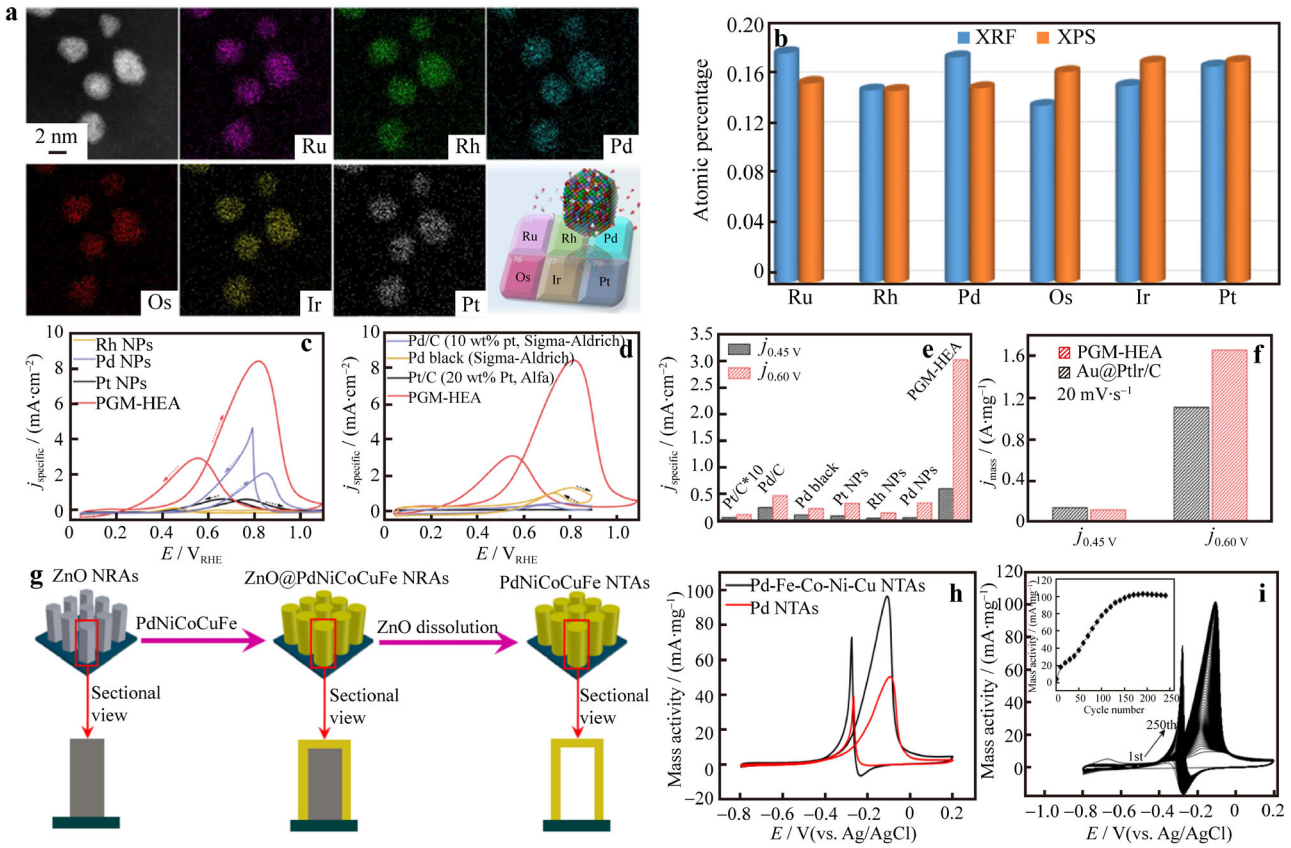

Fig. 2 **a** HAADF-STEM image with corresponding EDX maps and schematic diagram of PEG-HEA NPs; **b** composition analysis of PGM-HEA according to XRF and XPS; **c–f** EOR performances of PEG-HEA NPs and commercial catalysts. Reproduced with permission from Ref. [62]. Copyright 2020, American Chemical Society. **g** Illustration of preparing PdNiCoCuFe NTAs; **h** catalytic activity and **i** stability of PdNiCoCuFe NTAs tested in 0.5 mol·L^{-1} CH_3OH +1.0 mol·L^{-1} NaOH at 50 mV·s^{-1}. Reproduced with permission from Ref. [72]. Copyright 2014, Elsevier

potential to solve these issues. Rossmeisl and co-workers predicted that NM-HEAs could exhibit an excellent catalytic performance of ORR through density functional theory (DFT) calculated *OH and *O adsorption energies on random sites of IrPdPtRhRu HEAs surface [80]. The comparison between the adsorption energy calculated by DFT of *OH and * O and the predicted value of the model which uses the ordinary least squares algorithm is shown in Fig 3a, the accuracy of these predictions is very high, and the root mean square deviation (RMSD) of * OH and * O is only 0.063 eV. The surface of IrPdPtRhRu HEAs offered a near-continuum of adsorption energies and the adsorption energies can be tuned by changing the bulk composition to match the peak of the volcano curve. As shown in Fig. 3b, the adsorption energies and catalytic activity of IrPdPtRhRu HEAs changed with each element content tuning. When the contents of Ir, Pd, Pt, Rh and Ru are 10.2 at%, 32.0 at%, 9.3 at%, 19.3 at% and 28.9 at%, IrPdPtRhRu HEAs possessed a stable structure and showed the superior performance of ORR. Besides theoretical calculations, the advantages of NM-HEAs on ORR performance were also demonstrated by experiments [81, 82]. Yao et al. [83] reported a high-throughput synthesis of ultrafine and homogeneous NM-HEAs through composition design step and rapid thermal shock synthesis step (Fig. 3c). The components of HEAs can be tuned easily by this method and a series of PtPdRuRhIrFeCoNi alloys with various elemental compositions were prepared. After rapid electrochemical screening by using a scanning droplet cell, PtPdFeCoNi HEAs delivered enhanced catalytic properties of ORR (Fig. 3d–h). Qiu and co-workers fabricated a series nanoporous Pt-based HEAs with a low Pt content of 20 at%–30 at% through top-down dealloying method [84]. As a proof-of-concept application, these Pt-based HEAs were evaluated as electrocatalysts for ORR. Among these catalysts, np-Al–Cu–Ni–Pt–Mn HEAs showed the optimal catalytic activity, which is 16 times higher than that of Pt/C catalysts in mass activity. Based on the first-principles simulations, Mn combined with Ni, Cu and Al could effectively modify the electronic structure of Pt, leading to the excellent ORR performance of Al–Cu–Ni–Pt–Mn HEAs.

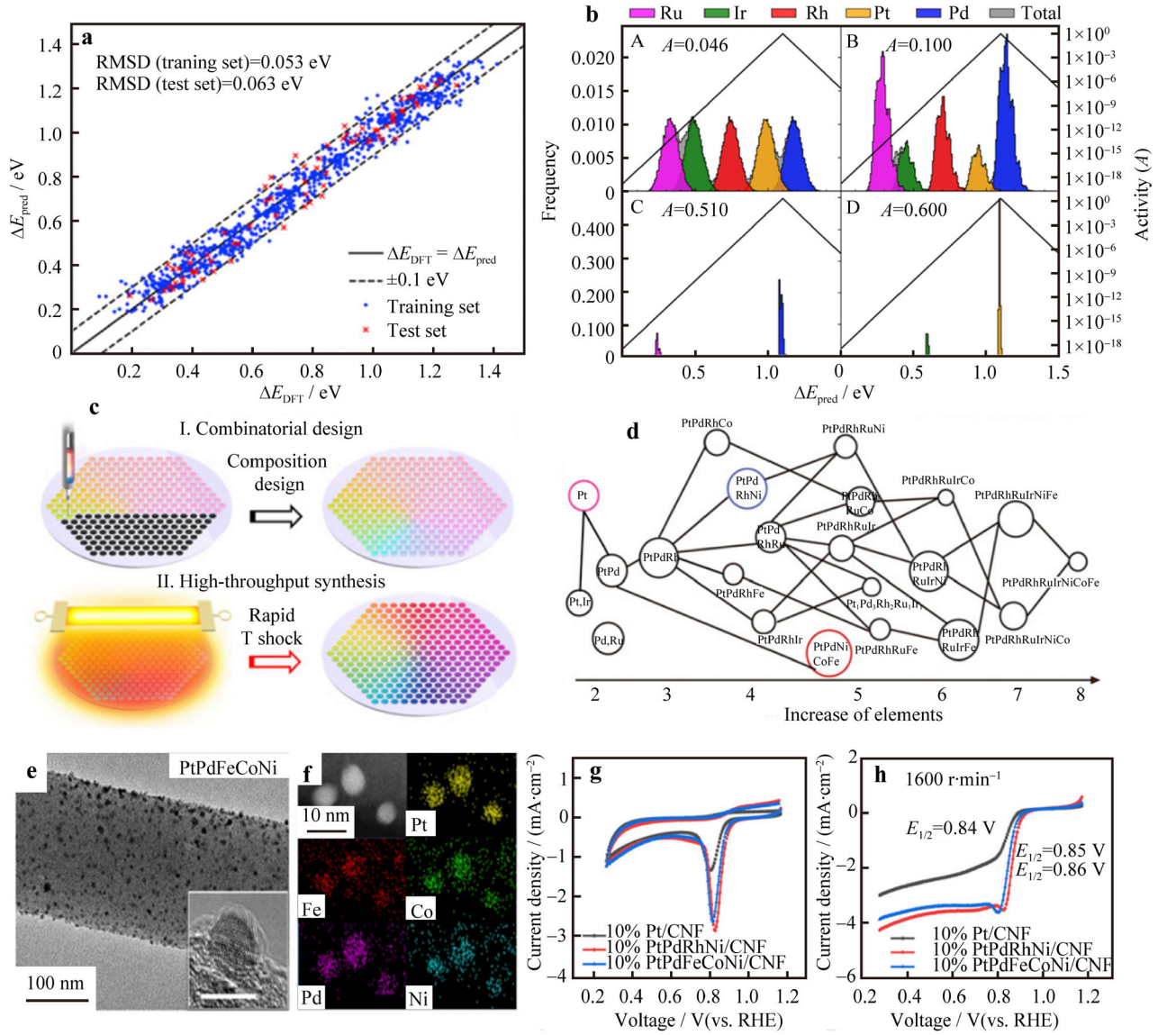

Fig. 3 **a** *OH adsorption on 871 symmetric 2×2 unit cells (blue dots) and tested on 76 asymmetric 3×4 unit cells (red crosses); **b** activities of Re-engineered Compositions of alloys. Reproduced with permission from Ref. [80]. Copyright 2019, Cell. **c** Schematic images of combinatorial and high-throughput fabrication of MMNCs; **d** ORR performance of various MMNCs, where size of these circles indicates magnitude of specific current at 0.45 V for ORR); **e** TEM image and **f** corresponding EDX maps of PtPdFeCoNi alloys; **g** cycle voltammograms and **h** linear-sweep voltammograms of these catalysts at 10 mV·s^{-1}. Reproduced with permission from Ref. [83]. Copyright 2020, National Academy of Sciences

3.3 Electrocatalytic HER

HER as a semireaction of electrochemical splitting of water has attracted wide attention in past decades to produce hydrogen energy, which is one of the most important clean energy in the future. To date, Pt is generally regarded as the most excellent catalysts for electrocatalytic HER in acidic environment, but the costliness and sluggish kinetics in alkaline electrolyte impede its practical utilization [85–89]. Recent reports showed that fabricating NM-HEAs catalysts could boost the HER performance both in acidic and alkaline solution as well as reduce the usage of Pt. Liu et al. [58] successfully prepared PtAuPdRhRu HEAs NPs through a facile ultrasonication-assisted method by means of the instantaneously massive energy generated by acoustic cavitation (Fig. 4a). Thanks to the strong synergistic effect between various elements and high entropy effect, PtAuPdRhRu HEAs NPs delivered a superior activity. The onset potential and Tafel slope of PtAuPdRhRu HEAs NPs reduced remarkably compared to those of other contrastive Pt-based catalysts (Fig. 4b). In addition, Wu et al. [90] fabricated IrPdPtRhRu HEAs NPs

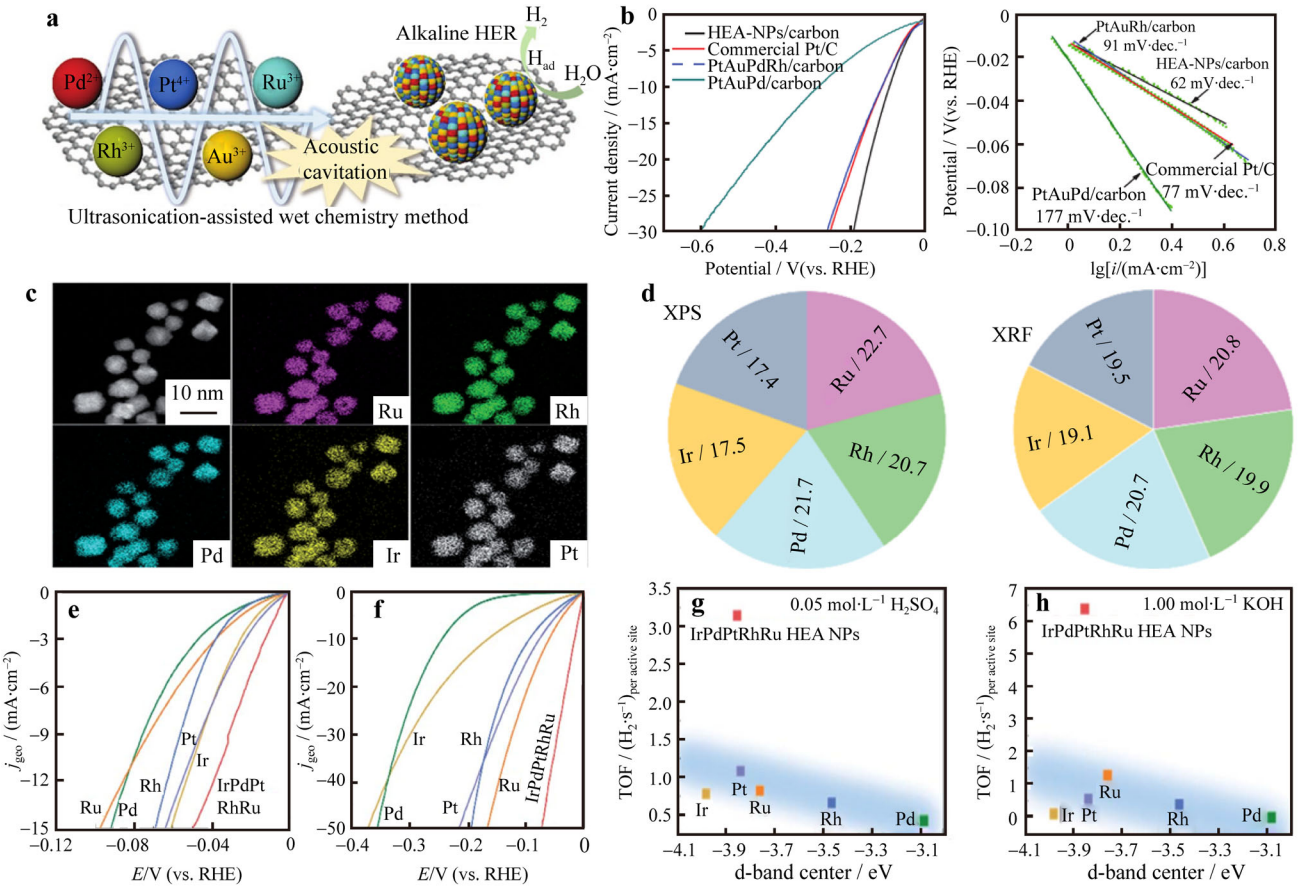

Fig. 4 **a** Schematic image of synthetic method and HER application for PtAuPdRhRu/C; **b** HER polarization curves and Tafel plots of various catalysts in 1.0 mol·L^{-1} KOH solution. Reproduced with permission from Ref. [58]. Copyright 2019, Wiley-VCH. **c** HAADF-STEM images and EDX-mapping of RuRhPdIrPt HEAs NPs; **d** component of RuRhPdIrPt HEAs NPs characterized by XPS and XRF; HER polarization curves of RuRhPdIrPt HEAs NPs and other monometallic catalysts in **e** 0.05 mol·L^{-1} H_2SO_4 and **f** 1.00 mol·L^{-1} KOH solution; interrelation between TOF values at 0.05 (vs. RHE) and d-band center in **g** 0.05 mol·L^{-1} H_2SO_4 and **h** 1.00 mol·L^{-1} KOH solution (d-band center relative to Fermi level). Reproduced with permission from Ref. [90]. Copyright 2020, Elsevier

with the average size of (5.5 ± 1.2) nm through co-reduction process of these five metal precursors in triethylene glycol solution at 230 °C, and the amount of each element is basically identical characterized by XPS and XRF (Fig. 4c, d). Especially, diverse local electronic structures on IrPdPtRhRu HEAs NPs caused by the random atomic configurations have been directly demonstrated by hard XPS. In the study of electrocatalytic HER performance, IrPdPtRhRu HEAs NPs exhibited outstanding activity both in acidic and alkaline solution (Fig. 4e, f). In order to prove whether the activity of IrPdPtRhRu HEA NPs is related to the adsorption energy of intermediate H species, the turnover frequency (TOF) value at 50 mV is plotted as a function of experimental d-band center which can reflect the metal–H binding of monometallic and most binary catalysts in solutions of 0.05 mol·L^{-1} H_2SO_4 and 1.0 mol·L^{-1} KOH (Fig. 4g, h). According to Fig. 4g, h, the TOF value of monometallic NPs is approximatively related to the d-band center, the deeper the d-band center is, the higher the activity is. However, it should be noted that the enhanced HER performances do not fit perfectly to the d-band theory all the time, suggesting that the relationship between electronic structure and HER performance of NM-HEAs is complex and needs to be further investigated.

3.4 Electrocatalytic OER

OER is the other semireaction of electrocatalytic water splitting process, which possesses a complex four-electron transfer process, leading to the high kinetic energy overpotential [91–97]. Although numerous excellent non-noble metal-based catalysts have been obtained and exhibited excellent OER performance, these electrocatalysts are generally not suitable to acidic solution. Ir, Ru and their oxides are still the most excellent electrocatalysts for the OER in acidic environment, as well as in alkaline electrolyte. Therefore, the content of Ir and Ru in electrocatalysts is highly desirable to reduce and the activity and

stability are wished to be further enhanced. Jin et al. [98] synthesized np-AlNiCoIrMo HEAs with uniform distribution of elements by a facile dealloy process (Fig. 5a, b). The atomic ratio of Ir in this np-AlNiCoIrMo HEAs is only ~20%, which is much lower than that of binary and ternary Ir-based alloys. Owing to the high-entropy effect and sluggish diffusion effect of HEA, np-AlNiCoIrMo HEAs show a record-high OER electrocatalytic activity in acidic solution as well as superior stability (Fig. 5c, d). As shown in Fig. 5d, the potential changes of np-AlNiCoIrMo, AlNiCoIrCu and AlNiCoIrNb samples are very small, about 11.5, 2.1 and 11.0 mV, respectively, while np-AlNiIr shows a sharp potential increase of about 70.3 mV at 60 $mA \cdot cm^{-2}$ after 7000 cycles. These results prove that the quinary HEAs have excellent durability. Based on the calculation of Ir–O band, the covalency of Ir–O bond could be increased through alloying Ir with Ni and Mo, leading to the outstanding OER performance (Fig. 5e). Moreover, beside HEAs, Glasscott et al. [57] showed a generalized platform for fabricating the noble metal-based high-

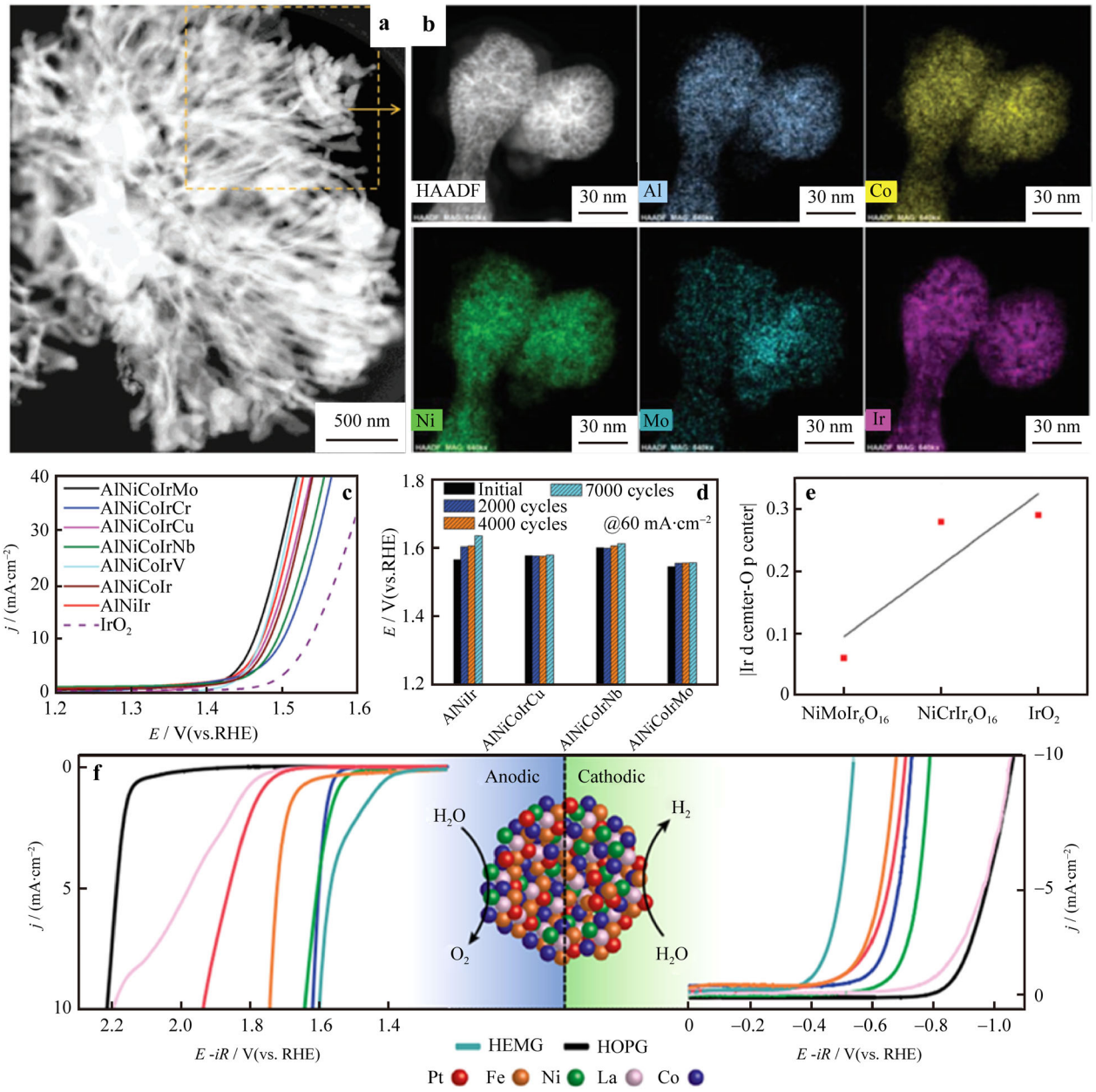

Fig. 5 **a** HAADF-STEM and **b** EDX-mapping images of np-AlNiCoIrMo HEAs; **c** OER polarization and **d** catalytic stability of Ir-based HEAs and IrO_2. **e** Difference of Ir d-band center and O p-band center for various catalysts. Reproduced with permission from Ref. [98]. Copyright 2019, Wiley-VCH. **f** Electrocatalytic evaluation of CoFeLaNiPt HEMG-NP electrocatalyst for HER and OER. Reproduced with permission from Ref. [57]. Copyright 2019, Nature Publishing Group

entropy metallic glasses, which were also containing disordered five or more equimolar components, but with amorphous microstructure. These novel catalytic materials exhibit excellent OER performance as well as HER due to the strong synergistic effect (Fig. 5f) and provide novel idea for designing advanced water splitting electrocatalysts.

3.5 Electrocatalytic CO_2RR

Electrocatalytic CO_2RR has been regarded as a promising technology for the proficient conversion of CO_2 into chemical fuels [99–106]. However, the high kinetic barriers, complex multielectron process and competition with HER in CO_2RR lead to the unsatisfactory activity and selectivity, which hinder its practical application. In previous reports, CO binding energy of metal electrocatalysts played a key role in tuning the activity and selectivity of CO_2RR. For instance, Au NPs as the electrocatalysts for CO_2RR could exhibit the superior activity due to the weak Au−CO binding energy, but the products are mainly CO. Cu NPs as the electrocatalysts could result in a variety of products including hydrocarbons and oxygenates due to the intermediate CO binding energy [107–111]. NM-HEAs hold a great potential as electrocatalysts for CO_2RR since the cocktail effect, high entropy effect, lattice distortion effect, phase structure and sluggish diffusion effect in HEAs could effectively modify the electronic structure and tune the CO binding energy. Rossmeisl and co-workers systematically calculated the CO and H adsorption energies on (111) surface sites of disordered AgAuCuPdPt HEAs with various components through combining DFT with supervised machine learning (Fig. 6a–f) [24]. The results demonstrated that optimizing the HEA compositions could increase the likelihood for sites with weak H adsorption and strong CO adsorption, which can suppress the competition of HER and enhance the reduction of CO. In an experimental attempt, Nellaiappan et al. [112] fabricated AuAgPtPdCu HEAs as a "single-atom catalyst" for the electrochemical reduction of CO_2 to reveal the advantages of HEAs catalysts toward CO_2RR (Fig. 6g–k). They find that redox-active Cu metal (Cu^{2+}/Cu^0) is the only activity site for electrocatalytic CO_2RR in AuAgPtPdCu HEAs, other metal elements only provide a synergistic effect. Different from the pure Cu catalysts, the products of CO_2 conversion are complete 100% gaseous at a lower potential on AuAgPtPdCu HEAs, and with an excellent stability. According to the free-energy calculations of intermediates, the destabilization of the $*OCH_3$ and stabilization of the *O on HEAs surface lead to the lower limiting potential. In addition, − 0.45 eV of free-energy adsorption of H is usually the thermoneutral value for efficient HER catalysts, resulting in the lower Faraday efficiency (FE) of H_2 than that of CH_4 and C_2H_4.

4 Summary and outlook

Noble metal-based catalysts have been investigated widely in electrocatalytic field. However, the high cost and unsatisfactory catalytic performance are still not effectively addressed. Recently, NM-HEAs have exhibited great promising to enhance the catalytic performance as well as decrease the usage of noble metal. In this review, the preparation methods of NM-HEAs have been systematically evaluated and the advantages of HEAs electrocatalysts including high entropy effect, cocktail effect, lattice distortion effect, phase structure and sluggish diffusion effect have been discussed. These characteristics could effectively modify the geometric/electronic structure of NM-HEAs. Moreover, recent progresses in NM-HEAs electrocatalysts for fuel cells, water splitting and CO_2 reduction have been summarized, with focus on the roles of high entropy effect, cocktail effect and lattice distortion effect in the enhancement of catalytic property. Although several significant efforts have been devoted to the exploitation of advanced NM-HEAs electrocatalysts for energy conversion. The research is still in the infant stage and many challenges and problems still need to be solved.

4.1 Facile preparation of NM-HEAs

Until so far, despite several different kinds of strategies have been developed to successfully synthesize NM-HEAs, the novel preparation method particularly easy-to-operation under ambient condition is highly desirable. Those methods mentioned in this review above either need specialized equipment (mechanical alloying, sputter deposition, spark discharge, etc.), or need to be operated in extreme condition (carbothermal shock synthesis, sputter deposition, etc.), such as high temperature of thousands degree or high vacuum. Additionally, the small preparation scale is also an issue needed to be addressed. Therefore, the simple, easy-to-operate and scale-up methods of fabricating NM-HEAs under facile conditions are imperative to develop.

4.2 Morphology-controlled synthesis of NM-HEAs

As is well known, the morphology of noble metal alloyed electrocatalysts has great influences on the catalytic performance. Various exposed facets possess different binding energies of intermediates, influencing the catalytic activity and stability. In the past decades, shape-controlled fabricating noble-based catalysts have been investigated in-

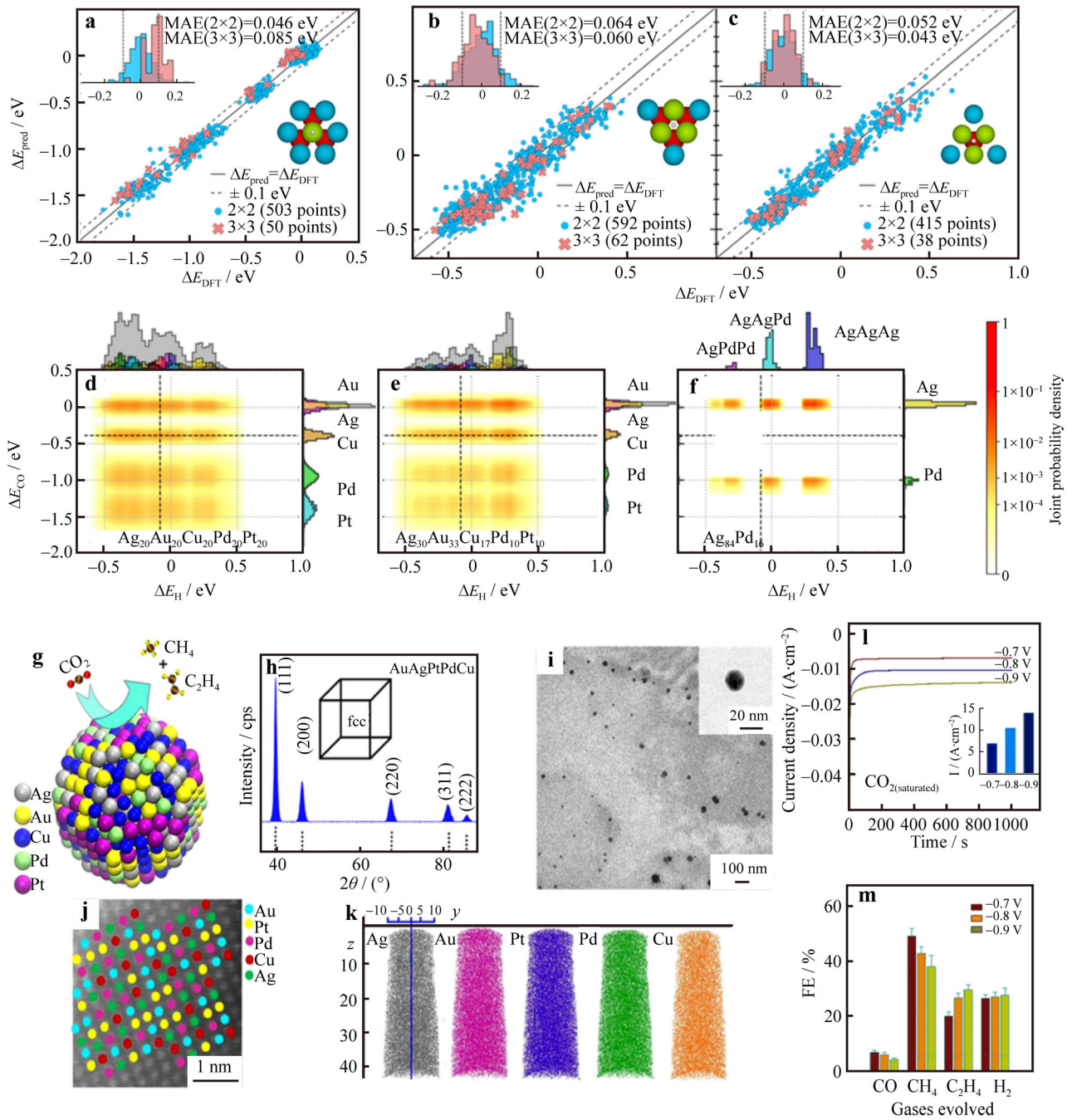

Fig. 6 GPR-predicted (ΔE_{pred}) versus DFT-calculated (ΔE_{DFT}) adsorption energies of AgAuCuPdPt for **a** on-top, **b** fcc-hollow H and **c** hcp-follow H, where blue represents data for 2 × 2 atoms slabs and red 3 × 3 atoms slabs; distributions of H and CO adsorption energies for AgAuCuPdPt **d** equimolar components, **e** optimal components and **f** locally optimal components without constraints. Reproduced with permission from Ref. [24]. Copyright 2020, American Chemical Society. **g** Schematic diagram, **h** XRD pattern, **i** TEM image, **j** HRTEM image and **k** atom probe microscope mapping image of AuAgPtPdCu NPs; **l** chronoamperometric test in CO_2-saturated solution at −0.7, −0.8 and −0.9 V for 1000 s; **m** Faradic efficiencies of different products. Reproduced with permission from Ref. [112]. Copyright 2020, American Chemical Society

depth and the structure-performance relationships in many electrocatalytic reactions have been gradually revealed [113]. For instance, concave nanocubic and tetrahexahedral noble-based NPs generally exposed high-index facets (HIFs), which usually enhanced the catalytic performance due to the low coordination numbers of surface atoms [114]. In addition, numerous state-of-art noble-based decahedrons and icosahedrons also exhibit superior

performance for electrocatalytic HER, ORR and CO_2RR due to the abundant twinned defects on the surface and the introduction of strain effect.

Fine controlling the nucleation/growth kinetics of metal alloyed NPs to desired shape is more difficult with the increase in compositional metals. Especially, NM-HEAs require five or more elements with equal content (or 5 at%–35 at%), leading to the greater difficulty. Therefore, morphology-controlled preparation of NM-HEAs remains a great challenge and is reported rarely. However, based on the shape-controlled synthesis of ternary and quaternary alloys reported previously, it is promising to fabricate NM-HEAs with definite morphology through fine-tuning the capping agents, reducing agents, shape-regulation agents and other control conditions.

4.3 Phase structure regulation of NM-HEAs

Phase structure has been regarded as the most significant structural parameter and played a crucial role in determining the catalytic property of HEAs. Especially, the unconventional phases of metal elements generally endow them with intriguing catalytic properties and innovative applications. 4H Au shows enhanced activity and higher ethylene selectivity in electrochemical CO_2 reduction compared to the traditional (face center cubic) fcc Au [115]. Fcc Ru NPs could exhibit superior electrocatalytic HER and OER performance than conventional (hexagonal close packed) hcp Ru catalysts [44]. CoNi NPs with fcc/hcp closest packing polymorphism interface significantly boost the HER activity than CoNi NPs with pure fcc or hcp structure. Therefore, fabricating NM-HEAs with unconventional phase structure or multiple phases has great potential to enhance the electrocatalytic performance and is full of challenges at the same time. In general, we believe that NM-HEAs provide a novel strategy to fabricate advanced electrocatalysts and will be applied widely in the further.

Acknowledgements This work was financially supported by the National Natural Science Foundation of China (Nos. 21706074 and 21972038), the Natural Science Foundation of Henan Province (No. 2023000410209), the Key Research and Promotion Project of Henan Province (Nos. 202102210261 and 202102310267) and the Top-notch Personnel Fund of Henan Agricultural University (No. 30500682).

References

[1] Kim BH, Heo J, Kim S, Reboul CF, Chun H, Kang D, Bae H, Hyun H, Lim J, Lee H, Han B, Hyeon T, Alivisatos AP, Ercius P, Elmlund H, Park J. Critical differences in 3D atomic structure of individual ligand-protected nanocrystals in solution. Science. 2020;368(6486):60.

[2] Qin Y, Zhang W, Guo K, Liu X, Liu J, Liang X, Wang X, Gao D, Gan L, Zhu Y, Zhang Z, Hu W. Fine-tuning intrinsic strain in penta-twinned Pt–Cu–Mn nanoframes boosts oxygen reduction catalysis. Adv Funct Mater. 2020;30(11):1910107.

[3] Nosheen F, Wasfi N, Aslam S, Tauseef A, Hussain S, Hussain N, Shah S, Shaheen N, Ashraf A, Zhu Y, Wang H, Ma J, Zhang Z, Hu W. Ultrathin Pd-based nanosheets: syntheses, properties and applications. Nanoscale. 2020;12(7):42.

[4] Liu H, Zhu Y, Ma J, Zhang Z, Hu W. Recent advances in Atomic-level engineering of nanostructured catalysts for electrochemical CO_2 reduction. Adv Funct Mater. 2020;30(17):1910534.

[5] Centi C. Smart catalytic materials for energy transition. SmartMat. 2020;1(1):e1005.

[6] Wang C, Yang C, Zhang Z. Unraveling molecular-level mechanisms of reactive facet of carbon nitride single crystals photocatalyzing overall water splitting. Rare Met. 2020;39(12):1353.

[7] Yang C, Nosheen F, Zhang Z. Recent progress in structural modulation of metal nanomaterials for electrocatalytic CO_2 reduction. Rare Met. 2020. https://doi.org/10.1007/s12598-020-01600-4.

[8] Liu M, Zhao Z, Duan X, Huang Y. Nanoscale structure design for high-performance Pt-based ORR catalysts. Adv Mater. 2019;31(6):1802234.

[9] Lei W, Xiao JL, Liu HP, Jia QL, Zhang HJ. Tungsten disulfide: synthesis and applications in electrochemical energy storage and conversion. Tungsten. 2020;2(3):217.

[10] Wang AL, Zhu L, Yun Q, Han S, Zeng L, Cao W, Meng X, Xia J, Lu Q. Bromide ions triggered synthesis of noble metal-based intermetallic nanocrystals. Small. 2020;16(40):2003782.

[11] Wang Y, Li X, Zhang M, Zhou Y, Rao D, Zhong C, Zhang J, Han X, Hu W, Zhang Y, Zaghib K, Wang Y, Deng Y. Lattice-strain engineering of homogeneous NiS Se core-shell nanostructure as a highly efficient and robust electrocatalyst for overall water splitting. Adv Mater. 2020;32(40):2000231.

[12] Jiang K, Zhao J, Wang H. Catalyst design for electrochemical oxygen reduction toward hydrogen peroxide. Adv Funct Mater. 2020;30(35):2003321.

[13] Zhang Z, Luo Z, Chen B, Wei C, Zhao J, Chen J, Zhang X, Lai Z, Fan Z, Tan C, Zhao M, Lu Q, Li B, Zong Y, Yan C, Wang G, Xu ZJ, Zhang H. One-pot synthesis of highly anisotropic five-fold-twinned PtCu nanoframes used as a bifunctional electrocatalyst for oxygen reduction and methanol oxidation. Adv Mater. 2016;28(39):8712.

[14] Qin Y, Zhang X, Dai X, Sun H, Yang Y, Li X, Shi Q, Gao D, Wang H, Yu N, Sun S. Graphene oxide-assisted synthesis of Pt-Co alloy nanocrystals with high-index facets and enhanced electrocatalytic properties. Small. 2016;12(4):524.

[15] Wang LP, Shen QX, Tian L, Yang N, Xie G, Li B. Preparation of PtCo composite nanowires and characterization of electrocatalytic performance for oxygen reduction reaction. Chin J Rare Met. 2019;43(4):367.

[16] Liu S, Hu Z, Wu Y, Zhang J, Zhang Y, Cui B, Liu C, Hu S, Zhao N, Han X, Cao A, Chen Y, Deng Y, Hu W. Dislocation-strained IrNi alloy nanoparticles driven by thermal shock for the hydrogen evolution reaction. Adv Mater. 2020;32(48):2006034.

[17] Cui X, Zhang Z, Gong Y, Saleem F, Chen B, Du Y, Lai Z, Yang N, Li B, Gu L, Zhang H. Defect-rich, candied Haws--shaped AuPtNi alloy nanostructures for highly efficient electrocatalysis. CCS Chem. 2020;2(1):24.

[18] Tu K, Tranca D, Rodríguez-Hernández F, Jiang K, Huang S, Zheng Q, Chen MX, Lu C, Su Y, Chen Z, Mao H, Yang C, Jiang J, Liang HW, Zhuang X. A novel heterostructure based on RuMo nanoalloys and N-doped carbon as an efficient

electrocatalyst for the hydrogen evolution reaction. Adv Mater. 2020;32(46):2005433.
[19] Duan SB, Wang RM. Nanomaterials composed of noble metals and transition metal compounds: interface structure control and in-situ characterization at atomic scale. Chin J Rare Met. 2019; 43(11):1179.
[20] Yang C, Zhu Y, Liu J, Qin Y, Wang H, Liu H, Chen Y, Zhang Z, Hu W. Defect engineering for electrochemical nitrogen reduction reaction to ammonia. Nano Energy. 2020;77:105126.
[21] Zhang Z, Liu G, Cui X, Chen B, Zhu Y, Gong Y, Saleem F, Xi S, Du Y, Borgna A, Lai Z, Zhang Q, Li B, Zong Y, Han Y, Gu L, Zhang H. Crystal phase and architecture engineering of Lotus-Thalamus-shaped Pt-Ni anisotropic superstructures for highly efficient electrochemical hydrogen evolution. Adv Mater. 2018;30(30):1801741.
[22] Chen Y, Cheng T, Goddard WA III. Atomistic explanation of the dramatically improved oxygen reduction reaction of jagged platinum nanowires, 50 times better than Pt. J Am Chem Soc. 2020;142(19):8625.
[23] Yeh JW, Chen SK, Lin SJ, Gan JY, Chin TS, Shun TT, Tsau CH, Chang SY. Nanostructured high-entropy alloys with multiple principal elements: novel alloy design concepts and outcomes. Adv Eng Mater. 2004;6(5):299.
[24] Pedersen J, Batchelor T, Bagger A, Rossmeisl J. High-entropy alloys as catalysts for the CO_2 and CO reduction reactions. ACS Catal. 2020;10(3):2169.
[25] Xin Y, Li S, Qian Y, Zhu W, Yuan H, Jiang P, Guo R, Wang L. High-entropy alloys as a platform for catalysis: progress, challenges, and opportunities. ACS Catal. 2020;10(19):11280.
[26] Yang T, Zhao YL, Tong Y, Jiao ZB, Wei J, Cai JX, Han XD, Chen D, Hu A, Kai JJ, Lu K, Liu Y, Liu CT. Multicomponent intermetallic nanoparticles and superb mechanical behaviors of complex alloys. Science. 2018;362(6417):933.
[27] Ma Y, Wang Q, Jiang B , Li C, Hao JM, Li X, Dong C, Nieh T. Controlled formation of coherent cuboidal nanoprecipitates in body-centered cubic high-entropy alloys based on Al_2(Ni, Co, Fe, Cr)$_{14}$ compositions. Acta Mater. 2018;147:213.
[28] Senkov O, Jensen J, Pilchak A, Miracle D, Fraser H. Compositional variation effects on the microstructure and properties of a refractory high-entropy superalloy AlMoNbTaTiZr. Mater Des. 2018;139:498.
[29] Liu SF, Wu Y, Wang HT, He JY, Liu JB, Chen CX, Liu XJ, Wang H, Lu ZP. Stacking fault energy of face-centered-cubic high entropy alloys. Intermetallics. 2018;93:269.
[30] Fu Z, Jiang L, Wardini JL, MacDonald BE, Wen H, Xiong W, Zhang D, Zhou Y, Rupert TJ, Chen W, Lavernia EJ. A high-entropy alloy with hierarchical nanoprecipitates and ultrahigh strength. Sci Adv. 2018;4(10):8712.
[31] Tomboc G, Kwon T, Joo J, Lee K. High entropy alloy electrocatalysts: a critical assessment of fabrication and performance. J Mater Chem A. 2020;8(3):14844.
[32] Luan HW, Shao Y, Li JF, Mao WL, Han ZD, Shao CL, Yao KF. Phase stabilities of high entropy alloys. Scr Mater. 2020; 179:40.
[33] Zhang W, Liaw PK, Zhang Y. Science and technology in high-entropy alloys. Sci China Mater. 2018;61(1):2.
[34] Miracle DB, Senkov ON. A critical review of high entropy alloys and related concepts. Acta Mater. 2017;122:448.
[35] Zhang Y, Zuo T, Tang Z, Gao MC, Dahmen KA, Liaw PK, Lu ZP. Microstructures and properties of high-entropy alloys. Prog Mater Sci. 2014;61:1.
[36] Yeh JW. Alloy design strategies and future trends in High-entropy alloys. JOM. 2013;65(12):1759.
[37] Wang L, Zeng Z, Gao W, Maxson T, Raciti D, Giroux M, Pan X, Wang C, Greeley J. Tunable intrinsic strain in two-dimensional transition metal electrocatalysts. Science. 2019;363(6429):870.
[38] Wang Y, Li X, Zhang M, Zhou Y, Rao D, Zhong C, Zhang J, Han X, Hu W, Zhang Y, Zaghib K, Wang Y, Deng Y. Lattice strain engineering of homogeneous $NiS_{0.5}Se_{0.5}$ core-shell nanostructure as a highly efficient and robust electrocatalyst for overall water splitting. Adv Mater. 2020;32(40):2000231.
[39] Li J, Sharma S, Wei K, Chen Z, Morris D, Lin H, Zeng C, Chi M, Yin Z, Muzzio M, Shen M, Zhang P, Peterson AA, Sun S. Anisotropic strain tuning of L10Ternary nanoparticles for oxygen reduction. J Am Chem Soc. 2020;142(45):19209.
[40] Strasser P, Koh S, Anniyev T, Greeley J, More K, Yu C, Liu Z, Kaya S, Nordlund D, Ogasawara H, Toney MF, Nilsson A. Lattice-strain control of the activity in dealloyed core–shell fuel cell catalysts. Nat Chem. 2010;2(6):454.
[41] Luo M, Guo S. Strain-controlled electrocatalysis on multimetallic nanomaterials. Nat Rev Mater. 2017;2(11):17059.
[42] Xia Z, Guo S. Strain engineering of metal-based nanomaterials for energy electrocatalysis. Chem Soc Rev. 2019;48(12):3265.
[43] Chang X, Zeng M, Liu K, Fu L. Phase engineering of High-entropy alloys. Adv Mater. 2020;32(14):1907226.
[44] Zhao M, Xia Y. Crystal-phase and surface-structure engineering of ruthenium nanocrystals. Nat Rev Mater. 2020;5(6):440.
[45] Liu W, Tong Y, Chen S, Xu W, Wu H, Zhao Y, Yang T, Wang X, Liu X, Kai J, Liu CT. Unveiling the electronic origin for pressure-induced phase transitions in high-entropy alloys. Matter. 2020;2(3):51.
[46] Ge Y, Huang Z, Ling C, Chen B, Liu G, Zhou M, Liu J, Zhang X, Cheng H, Liu G, Du Y, Sun C, Tan C, Huang J, Yin P, Fan Z, Chen Y, Yang N, Zhang H. Phase-selective epitaxial growth of heterophase nanostructures on unconventional 2H-Pd nanoparticles. J Am Chem Soc. 2020;142(44):18971.
[47] Yun Q, Lu Q, Li C, Chen B, Zhang Q, He Q, Hu Z, Zhang Z, Ge Y, Yang N, Ge J, He Y, Gu L, Zhang H. Synthesis of PdM (M = Zn, Cd, ZnCd) nanosheets with an unconventional face-centered tetragonal phase as highly efficient electrocatalysts for ethanol oxidation. ACS Nano. 2019;13(12):14329.
[48] Dwivedi A, Koch CC, Rajulapati KV. On the single phase fcc solid solution in nanocrystalline Cr-Nb-Ti-V-Zn high-entropy alloy. Mater Lett. 2016;183:44.
[49] Alivisatos AP. Future of nano letters early career board. Nano Lett. 2017;17(11):6507.
[50] Wu H, Huang S, Zhu C, Zhu H, Xie Z. Excellent mechanical properties of in-situ TiC/FeCrNiCu$V_{0.1}$ high entropy alloy matrix composites. Mater Lett. 2019;257:126729.
[51] Pan J, Dai T, Lu T, Ni X, Dai J, Li M. Microstructure and mechanical properties of $Nb_{25}Mo_{25}Ta_{25}W_{25}$ and Ti_8Nb_{23}-$Mo_{23}Ta_{23}W_{23}$ high entropy alloys prepared by mechanical alloying and spark plasma sintering. Mater Sci Eng A. 2018; 738:362.
[52] Zhao S, He L, Fan X, Liu C, Long J, Wang L, Chang H, Wang J, Zhang W. Microstructure and chloride corrosion property of nanocrystalline AlTiCrNiTa high entropy alloy coating on X80 pipeline steel. Surf Coat Technol. 2019;375:215.
[53] Yao Y, Huang Z, Xie P, Lacey SD, Jacob RJ, Xie H, Chen F, Nie A, Pu T, Rehwoldt M, Yu D, Zachariah MR, Wang C, Shahbazian-Yassar R, Li J, Hu L. Carbothermal shock synthesis of high-entropy-alloy nanoparticles. Science. 2018; 359(6383):1489.
[54] Jia YJ, Chen HN, Liang XD. Microstructure and wear resistance of CoCrNbNiW high-entropy alloy coating prepared by laser melting deposition. Rare Met. 2019;38(12):1153.
[55] Kumar N, Tiwary CS, Biswas K. Preparation of nanocrystalline high-entropy alloys via cryomilling of cast ingots. J Mater Sci. 2018;53(19):13411.

[56] Wu Q, Wang Z, He F, Wang L, Luo J, Li J, Wang J. High entropy alloys: from bulk metallic materials to nanoparticles. Metall Mater Trans A. 2018;49(10):4986.
[57] Glasscott MW, Pendergast AD, Goines S, Bishop AR, Hoang AT, Renault C, Dick JE. Publisher correction: electrosynthesis of high-entropy metallic glass nanoparticles for designer, multi-functional electrocatalysis. Nat Commun. 2019;10(1):3115.
[58] Liu M, Zhang Z, Okejiri F, Yang S, Zhou S, Dai S. Entropy-maximized synthesis of multimetallic nanoparticle catalysts via a ultrasonication-assisted wet chemistry method under ambient conditions. Adv Mater Interfaces. 2019;6(7):1900015.
[59] Qiu H, Fang G, Wen Y, Liu P, Xie G, Liu X, Sun S. Nanoporous high-entropy alloys for highly stable and efficient catalysts. J Mater Chem A. 2019;7(11):6499.
[60] Gao S, Hao S, Huang Z, Yuan Y, Han S, Lei L, Zhang X, Shahbazian-Yassar R, Lu J. Synthesis of high-entropy alloy nanoparticles on supports by the fast moving bed pyrolysis. Nat Commun. 2020;11(1):2016.
[61] Bondesgaard M, Broge NLN, Mamakhel A, Bremholm M, Iversen BB. General solvothermal synthesis method for complete solubility range bimetallic and high-entropy alloy nanocatalysts. Adv Funct Mater. 2019;29(50):1905933.
[62] Wu D, Kusada K, Yamamoto T, Toriyama T, Matsumura S, Kawaguchi S, Kubota Y, Kitagawa H. Platinum-group-metal high-entropy-alloy nanoparticles. J Am Chem Soc. 2020;142(32):13833.
[63] Paul MTY, Kim D. Saha M. Solvothermal synthesis method for complete solubility range bimetallic and high-entropy alloy nanocatalysts. Adv Funct Mater. 2019;29(50):1905933.
[64] Tang AY, Jankovic J, Crisci L, Pedram S. Comparison of planar and tubular flow field plates for proton exchange membrane fuel cells (PEMFCs) through Simulation S, Stumper J, Gates B D. patterning catalyst layers with microscale features by soft lithography techniques for proton exchange membrane fuel cells. ACS Appl Energy Mater. 2019;3(1):478.
[65] Zheng Z, Yang F, Lin C, Zhu F, Shen S, Wei G, Zhang J. Voltage cycling-induced Pt degradation in proton exchange membrane fuel cells: effect of cycle profiles. ACS Appl Mater Interfaces. 2020;12(31):35088.
[66] Liang Z, Song L, Deng S, Zhu Y, Stavitski E, Adzic RR, Chen J, Wang JX. Direct 12-electron oxidation of ethanol on a ternary Au(core)-PtIr(Shell) electrocatalyst. J Am Chem Soc. 2019;141(24):9629.
[67] Yang N, Zhang Z, Chen B, Huang Y, Chen J, Lai Z, Chen Y, Sindoro M, Wang AL, Cheng H, Fan Z, Liu X, Li B, Zong Y, Gu L, Zhang H. Synthesis of ultrathin PdCu alloy nanosheets used as a highly efficient electrocatalyst for formic acid oxidation. Adv Mater. 2017;29(29):1700769.
[68] Qiu HJ, Shen X, Wang JQ, Hirata A, Fujita T, Wang Y, Chen MW. Aligned nanoporous Pt–Cu bimetallic microwires with high catalytic activity toward methanol electrooxidation. ACS Catal. 2015;5(6):3779.
[69] Xu C, Hao Q, Duan H. Nanoporous PdPt alloy as a highly active electrocatalyst for formic acid oxidation. J Mater Chem A. 2014;2(23):8875.
[70] Zhang Y, Yuan X, Lyu F, Wang X, Jiang X, Cao M, Zhang Q. Facile one-step synthesis of PdPb nanochains for high-performance electrocatalytic ethanol oxidation. Rare Met. 2020;39(7):792.
[71] Gao D, Li S, Lv Y, Zhuo H, Zhao S, Song L, Yang S, Qin Y, Li C, Wei Q, Chen G. PtNi colloidal nanoparticle clusters: tuning electronic structure and boundary density of nanocrystal subunits for enhanced electrocatalytic properties. J Catal. 2019;376:87.
[72] Wang A, Wan H, Xu H, Tong Y, Li G. Quinary PdNiCoCuFe alloy nanotube arrays as efficient electrocatalysts for methanol oxidation. Electrochim Acta. 2014;127:448.
[73] Chen X, Si C, Gao Y, Frenzel J, Sun J, Eggeler G, Zhang Z. Multi-component nanoporous platinum–ruthenium–copper–osmium–iridium alloy with enhanced electrocatalytic activity towards methanol oxidation and oxygen reduction. J Power Sources. 2015;273:324.
[74] Xiong Y, Yang Y, DiSalvo FJ, Abruña HD. Synergistic bimetallic metallic organic framework-derived Pt–Co oxygen reduction electrocatalysts. ACS Nano. 2020;14(10):13069.
[75] Tao L, Huang B, Jin F, Yang Y, Luo M, Sun M, Liu Q, Gao F, Guo S. Atomic PdAu interlayer sandwiched into Pd/Pt core/shell nanowires achieves superstable oxygen reduction catalysis. ACS Nano. 2020;14(9):11570.
[76] Kwon H, Kabiraz MK, Park J, Oh A, Baik H, Choi S, Lee K. Dendrite-embedded platinum-nickel multiframes as highly active and durable electrocatalyst toward the oxygen reduction reaction. Nano Lett. 2018;18(5):2930.
[77] Chang F, Bai Z, Li M, Ren M, Liu T, Yang L, Zhong C, Lu J. Strain-modulated platinum-palladium nanowires for oxygen reduction reaction. Nano Lett. 2020;20(4):2416.
[78] Xiao M, Gao L, Wang Y, Wang X, Zhu J, Jin Z, Liu C, Chen H, Li G, Ge J, He Q, Wu Z, Chen Z, Xing W. Engineering energy level of metal center: Ru single-atom site for efficient and durable oxygen reduction catalysis. J Am Chem Soc. 2019;141(50):19800.
[79] Gao L, Li X, Yao Z, Bai H, Lu Y, Ma C, Lu S, Peng Z, Yang J, Pan A, Huang H. Unconventional p–d hybridization interaction in PtGa ultrathin nanowires boosts oxygen reduction electrocatalysis. J Am Chem Soc. 2019;141(45):18083.
[80] Batchelor TAA, Pedersen JK, Winther SH, Castelli IE, Jacobsen KW, Rossmeisl J. High-entropy alloys as a discovery platform for electrocatalysis. Joule. 2019;3(3):834.
[81] Wang S, Xin H. Predicting catalytic activity of high-entropy alloys for electrocatalysis. Chem. 2019;5(3):502.
[82] Wu D, Kusada K, Kitagawa H. Recent progress in the structure control of Pd–Ru bimetallic nanomaterials. Sci Technol Adv Mater. 2016;17(1):583.
[83] Yao Y, Huang Z, Li T, Wang H, Liu Y, Stein HS, Mao Y, Gao J, Jiao M, Dong Q, Dai J, Xie P, Xie H, Lacey SD, Takeuchi I, Gregoire JM, Jiang R, Wang C, Taylor AD, Shahbazian-Yassar R, Hu L. High-throughput, combinatorial synthesis of multimetallic nanoclusters. PNAS. 2020;117(12):6316.
[84] Li S, Tang X, Jia H, Li H, Xie G, Liu X, Lin X, Qiu H. Nanoporous high-entropy alloys with low Pt loadings for high-performance electrochemical oxygen reduction. J Catal. 2020;383:164.
[85] Yin H, Zhao S, Zhao K, Muqsit A, Tang H, Chang L, Zhao H, Gao Y, Tang Z. Ultrathin platinum nanowires grown on single-layered nickel hydroxide with high hydrogen evolution activity. Nat Commun. 2015;6(1):6430.
[86] Liu G, Zhou W, Chen B, Zhang Q, Cui X, Li B, Lai Z, Chen Y, Zhang Z, Gu L, Zhang H. Synthesis of RuNi alloy nanostructures composed of multilayered nanosheets for highly efficient electrocatalytic hydrogen evolution. Nano Energy. 2019;66:104173.
[87] Ledezma-Yanez I, Wallace WDZ, Sebastián-Pascual P, Climent V, Feliu JM, Koper MTM. Interfacial water reorganization as a pH-dependent descriptor of the hydrogen evolution rate on platinum electrodes. Nat Energy. 2017;2(4):17031.
[88] Hua W, Sun H, Xu F, Wang J. A review and perspective on molybdenum-based electrocatalysts for hydrogen evolution reaction. Rare Met. 2020;39(4):335.
[89] Fan Z, Luo Z, Huang X, Li B, Chen Y, Wang J, Hu Y, Zhang H. Synthesis of 4H/fcc noble multimetallic nanoribbons for

electrocatalytic hydrogen evolution reaction. J Am Chem Soc. 2016;138(4):1414.
[90] Wu D, Kusada K, Yamamoto T, Toriyama T, Matsumura S, Gueye I, Seo O, Kim J, Hiroi S, Sakata O, Kawaguchi S, Kubota Y, Kitagawa H. On the electronic structure and hydrogen evolution reaction activity of platinum group metal-based high-entropy-alloy nanoparticles. Chem Sci. 2020. https://doi.org/10.1039/d0sc02351e.
[91] Li X, Zhu P, Li Q, Xu Y, Zhao Y, Pang H. Nitrogen-, phosphorus-doped carbon–carbon nanotube CoP dodecahedra by controlling zinc content for high-performance electrocatalytic oxygen evolution. Rare Met. 2020;39(6):680.
[92] Fu L, Zeng X, Cheng G, Luo W. IrCo nanodendrite as an efficient bifunctional electrocatalyst for overall water splitting under acidic conditions. ACS Appl Mater, Interfaces. 2018; 10(30):24993.
[93] Kwon T, Hwang H, Sa YJ, Park J, Baik H, Joo SH, Lee K. Cobalt assisted synthesis of IrCu hollow octahedral nanocages as highly active electrocatalysts toward oxygen evolution reaction. Adv Funct Mater. 2017;27(7):1604688.
[94] Li J, Chu D, Dong H, Baker DR, Jiang R. Boosted oxygen evolution reactivity by igniting double exchange interaction in spinel oxides. J Am Chem Soc. 2019;142(1):50.
[95] Cao L, Luo Q, Chen J, Wang L, Lin Y, Wang H, Liu X, Shen X, Zhang W, Liu W, Qi Z, Jiang Z, Yang J, Yao T. Dynamic oxygen adsorption on single-atomic ruthenium catalyst with high performance for acidic oxygen evolution reaction. Nat Commun. 2019;10(1):4849.
[96] Stevens MB, Enman LJ, Batchellor AS, Cosby MR, Vise AE, Trang CDM, Boettcher SW. Measurement techniques for the study of thin film heterogeneous water oxidation electrocatalysts. Chem Mater. 2016;29(1):120.
[97] Shi Q, Zhu C, Du D, Lin Y. Robust noble metal-based electrocatalysts for oxygen evolution reaction. Chem Soc Rev. 2019;48(12):3181.
[98] Jin Z, Lv J, Jia H, Liu W, Li H, Chen Z, Lin X, Xie G, Liu X, Sun S, Qiu HJ. Nanoporous Al-Ni-Co-Ir-Mo high-entropy alloy for record-high water splitting activity in acidic environments. Small. 2019;15(47):1904180.
[99] Birdja YY, Pérez-Gallent E, Figueiredo MC, Göttle AJ, Calle-Vallejo F, Koper MTM. Advances and challenges in understanding the electrocatalytic conversion of carbon dioxide to fuels. Nat Energy. 2019;4(9):732.
[100] Kumar N, Mukherjee S, Bezrukov A, Vandichel M, Shivanna M, Sensharma D, Bajpai A, Gasocon V, Otake K, Kitagawa S, Zaworotko M. A square lattice topology coordination network that exhibits highly selective C_2H_2/CO_2 separation performance. SmartMat. 2020;1(1):e1008.
[101] Zhu JY, Liang F, Yao YC, Ma WH, Yang B, Dai YN. Preparation and application of metal organic frameworks derivatives in electro-catalysis. Chin J Rare Metals. 2019; 43(2):186.
[102] Dinh C, García De Arquer FP, Sinton D, Sargent EH. High rate, selective, and stable electroreduction of CO_2 to CO in basic and neutral media. ACS Energy Lett. 2018;3(11):2835.
[103] Geng Z, Kong X, Chen W, Su H, Liu Y, Cai F, Wang G, Zeng J. Oxygen vacancies in ZnO nanosheets enhance CO_2 electrochemical reduction to CO. Angew Chem Int Ed. 2018; 57(21):6054.
[104] He R, Zhang A, Ding Y, Kong T, Xiao Q, Li H, Liu Y, Zeng J. Achieving the widest range of syngas proportions at high current density over cadmium sulfoselenide nanorods in CO_2 electroreduction. Adv Mater. 2018;30(7):1705872.
[105] Wang X, Araújo J, Ju W, Bagger A, Schmies H, Kühl S, Rossmeisl J, Peter S. Mechanistic reaction pathways of enhanced ethylene yields during electroreduction of CO_2–CO co-feeds on Cu and Cu-tandem electrocatalysts. Nat Nanotechnol. 2019;14(5):1063.
[106] Li H, Wang L, Dai Y, Pu Z, Lao Z, Chen Y, Wang M, Zheng X, Zhu J, Zhang W, Si R, Ma C, Zeng J. Synergetic interaction between neighbouring platinum monomers in CO_2 hydrogenation. Nat Nanotechnol. 2018;13(5):411.
[107] Li YC, Wang Z, Yuan T, Nam D, Luo M, Wicks J, Chen B, Li J, Li F, de Arquer FPG, Wang Y, Dinh C, Voznyy O, Sinton D, Sargent EH. Binding site diversity promotes CO_2 electroreduction to ethanol. J Am Chem Soc. 2019;141(21):8584.
[108] Kibria MG, Edwards JP, Gabardo CM, Dinh CT, Seifitokaldani A, Sinton D, Sargent EH. Electrochemical CO_2 reduction into chemical feedstocks: from mechanistic electrocatalysis models to system design. Adv Mater. 2018;31(31):1807166.
[109] Nitopi S, Bertheussen E, Scott SB, Liu X, Engstfeld AK, Horch S, Seger B, Stephens IEL, Chan K, Hahn C, Nørskov JK, Jaramillo TF, Chorkendorff I. Progress and perspectives of electrochemical CO_2 reduction on copper in aqueous electrolyte. Chem Rev. 2019;119(12):7610.
[110] Zheng Y, Vasileff A, Zhou X, Jiao Y, Jaroniec M, Qiao S. Understanding the roadmap for electrochemical reduction of CO_2 to multi-carbon oxygenates and hydrocarbons on copper-based catalysts. J Am Chem Soc. 2019;141(19):7646.
[111] Yang C, Li S, Zhang Z, Wang H, Liu H, Jiao F, Guo Z, Zhang X, Hu W. Organic-inorganic hybrid nanomaterials for electrocatalytic CO_2 reduction. Small. 2020;16(29):2001847.
[112] Nellaiappan S, Katiyar NK, Kumar R, Parui A, Malviya KD, Pradeep KG, Singh AK, Sharma S, Tiwary CS, Biswas K. High-entropy alloys as catalysts for the CO_2 and CO reduction reactions: experimental realization. ACS Catal. 2020;10(6): 3658.
[113] Li XY, Qu JK, Yin HY. Electrolytic alloy-type anodes for metal-ion batteries. Rare Met. 2020. https://doi.org/10.1007/s12598-020-01537-8.
[114] Xiao C, Lu BA, Xue P, Tian N, Zhou Z, Lin X, Lin WF, Sun SG. High-index-facet- and high-surface-energy nanocrystals of metals and metal oxides as highly efficient catalysts. Joule. 2020. https://doi.org/10.1016/j.joule.2020.10.002.
[115] Wang Y, Li C, Fan Z, Chen Y, Li X, Cao L, Wang C, Wang L, Su D, Zhang H, Mueller T, Wang C. Undercoordinated active sites on 4H gold nanostructures for CO_2 reduction. Nano Lett. 2020;20(11):8074.

Yu-Chen Qin is currently a professor in College of Sciences, Henan Agricultural University. He received the Ph.D. degree from China University of Petroleum (Beijing) in 2016. His current research interests are metal-based electrocatalysts, electrocatalysis and photoelectrocatalysis.